



HAL
open science

The high-conductance state of neocortical neurons in vivo

Alain Destexhe, Michael Rudolph, Denis Paré

► **To cite this version:**

Alain Destexhe, Michael Rudolph, Denis Paré. The high-conductance state of neocortical neurons in vivo. *Nature Reviews Neuroscience*, 2003, 4 (9), pp.739-51. 10.1038/nrn1198 . hal-00299172

HAL Id: hal-00299172

<https://hal.science/hal-00299172>

Submitted on 28 Apr 2022

HAL is a multi-disciplinary open access archive for the deposit and dissemination of scientific research documents, whether they are published or not. The documents may come from teaching and research institutions in France or abroad, or from public or private research centers.

L'archive ouverte pluridisciplinaire **HAL**, est destinée au dépôt et à la diffusion de documents scientifiques de niveau recherche, publiés ou non, émanant des établissements d'enseignement et de recherche français ou étrangers, des laboratoires publics ou privés.



Distributed under a Creative Commons Attribution - NonCommercial 4.0 International License

THE HIGH-CONDUCTANCE STATE OF NEOCORTICAL NEURONS *IN VIVO*

Alain Destexhe*, Michael Rudolph* and Denis Paré‡

Intracellular recordings *in vivo* have shown that neocortical neurons are subjected to an intense synaptic bombardment in intact networks and are in a ‘high-conductance’ state. *In vitro* studies have shed light on the complex interplay between the active properties of dendrites and how they convey discrete synaptic inputs to the soma. Computational models have attempted to tie these results together and predicted that high-conductance states profoundly alter the integrative properties of cortical neurons, providing them with a number of computational advantages. Here, we summarize results from these different approaches, with the aim of understanding the integrative properties of neocortical neurons in the intact brain.

One of the most fascinating characteristics of the cerebral cortex is its extremely dense connectivity: each pyramidal neuron receives between 5,000 and 60,000 synaptic contacts. A large part of this connectivity originates from the cortex itself^{1,2}, but inputs are also received from subcortical structures, such as the brainstem and thalamus. In awake animals, neurons in these structures have high spontaneous firing rates^{3,4}. One might therefore expect that in intact networks, at any given time, many synaptic inputs onto a single neuron are simultaneously active. In keeping with this, intracellular recordings in awake animals have revealed that cortical neurons are subjected to an intense synaptic bombardment and, as a result, are more depolarized and have a lower input resistance⁵⁻⁷ than neurons in brain slices kept *in vitro*. However, how the ‘high-conductance state’ caused by this continuous synaptic chatter affects neuronal dynamics, and in particular neuronal responsiveness, remains unclear.

To evaluate the integrative properties of pyramidal neurons during high-conductance states, *in vivo* approaches are insufficient. They have the advantage of an intact network, but do not allow us to control synaptic inputs with sufficient precision. Such control is easier to achieve in brain slices kept *in vitro*, but the inherent network limitations of slices severely reduce spontaneous synaptic activity. Nevertheless, visually guided patch-clamp recordings and microfluorometry

have allowed important advances in the characterization of synaptic integration in cortical neurons⁸. These advances include precise measurements of the density and distribution of voltage-dependent channels in dendrites⁹, the characterization of dendritic spikes¹⁰ and sophisticated models of synaptic integration¹¹⁻¹³.

Clearly, the presence of voltage-dependent channels in dendrites and their ability to produce regenerative events influences the integrative properties of pyramidal neurons. However, because network activity might affect the integrative properties of cortical neurons (a theme proposed in theoretical studies almost 30 years ago^{14,15}), computational methods are needed to integrate the results of *in vivo* and *in vitro* experiments. Theoretical models have provided several predictions about the computational properties of neurons in high-conductance states¹⁵⁻¹⁸. They will be reviewed here.

We will start by providing an overview of the electrophysiological properties of cortical neurons during high-conductance states *in vivo*. Next, we will review *in vitro* findings regarding the distribution of voltage-gated channels and how they affect dendritic processing. We then will show how computational models have attempted to tie these *in vivo* and *in vitro* observations together and have pointed towards a number of computational principles for high-conductance states. We conclude by reviewing how *in vivo* and *in vitro* approaches can be merged using dynamic-clamp

*Integrative and Computational Neuroscience Unit (UNIC), CNRS, 1 Avenue de la Terrasse, 91198 Gif-sur-Yvette, France.
‡Center for Molecular and Behavioral Neuroscience, Rutgers University, Newark, New Jersey 07102, USA.
Correspondence to A.D.
e-mail: destexhe@iaf.cnrs-gif.fr
doi:10.1038/nrn1198

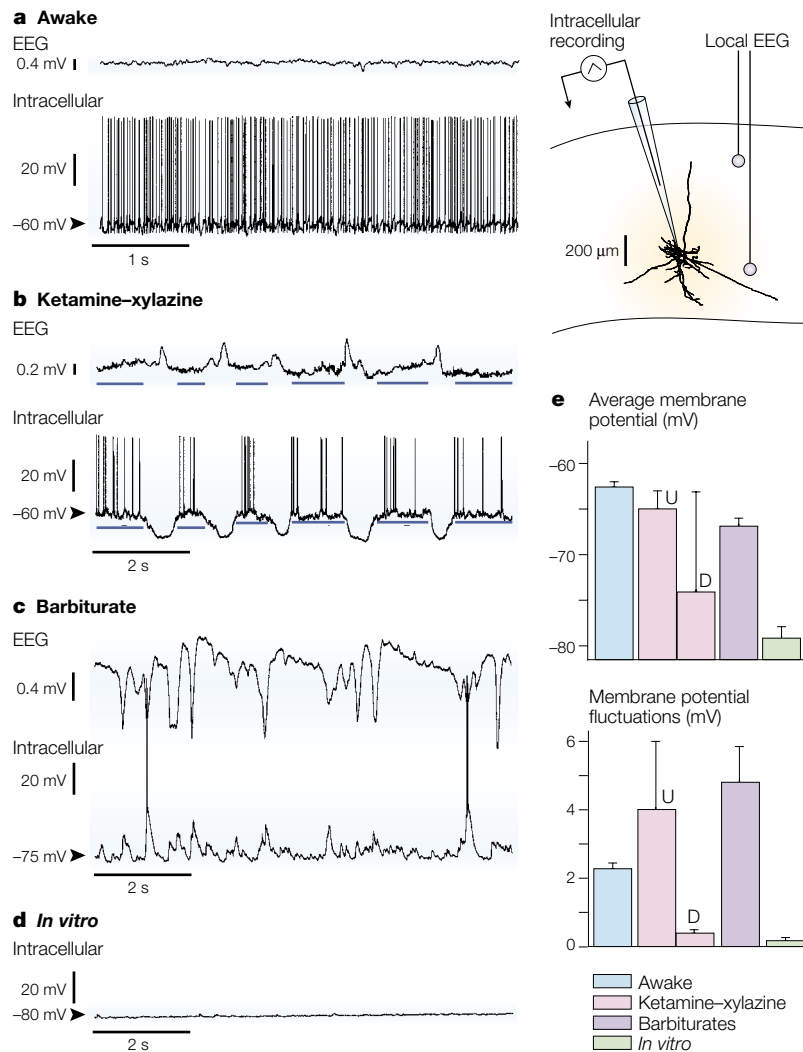


Figure 1 | Intracellular and electroencephalogram (EEG) recordings during different states of activity. Parallel intracortical EEG and intracellular recordings are compared across different cortical states. **a** | Awake animals: the EEG is desynchronized and the intracellular recording is characterized by a depolarized and highly fluctuating membrane potential that is associated with irregular firing. **b** | Under ketamine-xylazine anaesthesia, the EEG oscillates between two phases: desynchronized periods (up states, U; indicated by bars) with fast irregular EEG oscillations; and slow waves, during which fast EEG activities are absent or strongly reduced (down states, D). During the desynchronized periods (bars), the membrane potential is depolarized and highly fluctuating, whereas it is hyperpolarized during slow waves. **c** | Barbiturate anaesthesia: the EEG displays slow waves, whereas the intracellular signal consists of depolarized bursts riding on a hyperpolarized level. **d** | *In vitro* recordings are obtained in cortical slices using sharp electrodes. In this case, the network activity was reduced, as shown by the quiescent intracellular signal, which shows only discrete synaptic events. **e** | Comparison of the average value $\langle V_m \rangle$ and standard deviation σ_v of the membrane potential across different states. Panel **a** reproduced, with permission, from REF. 7 © (2001) American Physiological Society; Panel **b** reproduced, with permission, from REF. 17 © (1999) American Physiological Society; Panels **c** and **d** reproduced, with permission, from REF. 23 © (1998) American Physiological Society.

INPUT RESISTANCE
The voltage change elicited by the injection of current into a cell, divided by the amount of current injected.

experiments, in which computer-generated high-conductance states are used to study the effects of synaptic bombardment on synaptic integration *in vitro*. The aim of this review is to show that only through a tight combination of different approaches will we be able to understand synaptic integration in cerebral cortex during activated states.

High-conductance states *in vivo*

We start by describing the *in vivo* characterization of the activity of cortical neurons in awake animals, as well as in different states of anaesthesia. In particular, we focus on ‘activated’ states, which have electrophysiological characteristics close to those seen in the awake state.

The first intracellular recordings of central neurons date back to the middle of the last century, and were obtained in motor neurons of the cat spinal cord *in vivo*¹⁹. Since then, such recordings have been obtained in nearly all cortical regions. For technical reasons (such as mechanical stability), these recordings were usually performed in deeply anaesthetized animals, most commonly under barbiturate anaesthesia. Unfortunately, barbiturates profoundly depress cortical excitability, leading to an electroencephalographic (EEG) pattern akin to that seen during slow-wave sleep. Indeed, in barbiturate-anaesthetized animals, the EEG is dominated by slow waves of large amplitude that are associated with a synchronized burst-silence firing pattern in most cortical neurons. This is in contrast to activated states, during which the EEG shows low-amplitude fast activity (‘desynchronized EEG’), associated with asynchronous and irregular firing⁴.

To characterize cortical neurons during EEG-activated states, it is necessary to perform intracellular measurements in parallel with EEG recordings. Unfortunately, few such parallel measurements have been reported. FIGURE 1 shows typical examples of intracellular and EEG recordings during different states of activity, including awake animals (FIG. 1a), those under ketamine-xylazine anaesthesia (KX; FIG. 1b) and animals under barbiturate anaesthesia (FIG. 1c). In each case, the recorded activity contrasts with the relative quiescence that is usually seen in intracellularly-recorded neurons in cortical slices kept *in vitro* (FIG. 1d).

There have been few studies based on stable intracellular recordings in waking animals^{5-7,20,21}. Nevertheless, these studies described cortical neurons as having a low INPUT RESISTANCE (5–40 MΩ) and a depolarized membrane potential (around -60 mV) that fluctuates markedly ($\sigma_v = 2-6$ mV), causing irregular and tonic discharges in the 5–40-Hz frequency range⁷ (FIG. 1a). Differences in input resistance were also observed, depending on the behavioural state (wakefulness, slow-wave sleep or paradoxical sleep⁷), but in most cases, input resistance values were low compared to those reported *in vitro*^{22,23}. The results were the same irrespective of the cortical area^{5-7,20,21}. Input resistance measurements cannot be compared from one study to the next for several reasons. First, they depend on the electrode shape and impedance, which vary between laboratories. Second, in the case of data for unanaesthetized animals, these measurements depend on the behaviour of these animals. For instance, the relatively high input resistance reported in REF. 7 is based on data obtained during quiet wakefulness, which is presumably associated with lower levels of synaptic bombardment compared with active waking. However, values obtained in the same laboratory (FIG. 1b-d; KX, barb and *in vitro* in FIG. 2d) are comparable if they were obtained in the same cell type (the values

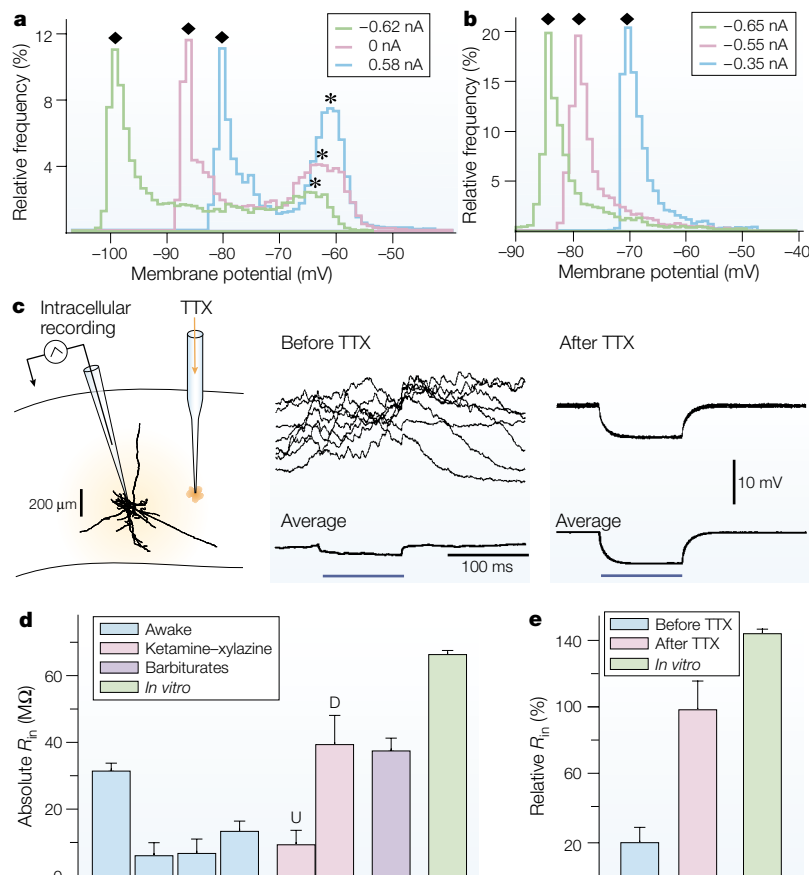


Figure 2 | Conductance measurements during different states of activity.

a | Ketamine-xylazine (KX) anaesthesia: membrane potential distributions at different direct current levels. The hyperpolarized (diamonds) and depolarized (asterisks) peaks correspond to the two states of the membrane (down and up states, respectively; see Fig. 1b). Current injection has less effect on the peak of the up state than the down state, indicating a lower input resistance in the up state. **b** | Barbiturate anaesthesia: same procedure as in **a**. In this case, the distribution of membrane potential is closer to the down state of KX anaesthesia shown in **a**. **c** | Suppression of network activity using microperfusion of tetrodotoxin (TTX). The scheme (left) illustrates the experimental setup; a microperfusion pipette was used to infuse TTX into the cortex *in vivo*. Middle panel: individual (top) and averaged (bottom) responses to injection of hyperpolarizing current pulses during the up state of KX. Right panel: responses to the same current pulse obtained in the same neuron after suppression of network activity by TTX. In this case, the input resistance and membrane time constant were about fivefold larger than in the up state. The post-TTX input resistance was similar to *in vitro* measurements using similar recording electrodes. **d** | Absolute value of input resistance (R_{in}) measurements in different studies. In awake animals, from left to right, data from REFS 7,5,20,6; KX data from REFS 17,23; barbiturate and *in vivo* data from REF. 23. **e** | Relative values of the input resistance measurements in the same cells before and after TTX. **a** and **b** reproduced, with permission, from REF. 23 © (1998) Americal Physiological Society; **c** and **e** reproduced, with permission, from REF. 17 © (1999) Americal Physiological Society.

before and after tetrodotoxin (TTX) in FIG. 2c,e were from the same cells).

Similar findings were reported using anaesthetics such as KX or urethane. In low doses, these anaesthetics produce alternating periods of activity and quiescence, often referred to as up and down states, respectively (FIG. 1b). During the up state (FIG. 1b, bars), which is associated with desynchronized fast EEG activity, cortical neurons are depolarized, fire spontaneously and have a low input resistance^{17,23,24}, similar to cortical neurons in awake animals. During the down state, when fast EEG activity is reduced, cortical neurons have a more stable and

hyperpolarized membrane potential (around -90 mV) and a higher input resistance (39 ± 9 M Ω , compared with 9.3 ± 4.3 M Ω for the up state). Stimulation of the brainstem ascending systems that maintain the waking state elicits a prolonged up state with a desynchronized EEG in animals anaesthetized with KX²⁵ or urethane²⁶. A similar pattern is seen in unanaesthetized animals during the transition from slow-wave sleep to wakefulness (see fig. 9 in REF. 7). These observations support the idea that such up states represent network states similar to wakefulness.

By contrast, barbiturate anaesthesia produces a state of reduced cortical activity (FIG. 1c) in which neurons fire at low rates. Conductance analyses show that barbiturates induce a state of lower global conductance compared with KX. For instance, FIG. 2a and FIG. 2b compare the effect of constant current injection in KX and barbiturate anaesthesia. In FIG. 2a, the voltage distribution shows two peaks, typical of the up and down states of KX. Current injection has a much larger effect on the down state than the up state, showing that there is a reduced conductance in the down state. Interestingly, the distributions obtained under barbiturate anaesthesia (FIG. 2b) are similar to the down states of KX.

In epochs of irregular fast EEG activity, as seen in waking and the up state of KX anaesthesia, cortical neurons have a low input resistance, are depolarized, experience continuous membrane potential fluctuations and fire spontaneously at rest. We will refer to this condition as the ‘high-conductance’ state of cortical neurons. This state differs markedly from that seen *in vitro*, where cortical cells lack spontaneous firing, and have a high input resistance and a hyperpolarized membrane potential, showing only discrete synaptic events (FIG. 1d).

To investigate the contribution of synaptic activity to high-conductance states, the same intracellularly recorded neurons were compared before and after suppression of network activity by microperfusion of the Na^+ -channel blocker TTX *in vivo*²³. TTX microperfusion produced a membrane hyperpolarization, an increased input resistance and a marked stabilization of the membrane potential (FIG. 2c–e). After TTX application *in vivo*, the membrane potential and input resistance of cortical cells were similar to those seen *in vitro* using the same type of electrodes²³. These results indicate that increased cell damage by intracellular electrodes *in vivo* does not account for the differences between *in vivo* and *in vitro* results. Rather, these experiments indicate that the depolarized level and the low input resistance of cortical neurons *in vivo* are mostly due to spontaneous synaptic activity (computational models indicate that less than 10% of the input resistance is due to activation of voltage-dependent channels¹⁷).

Consistent with this, the effect of TTX on the input resistance of cortical cells was greater in experiments conducted under KX than under barbiturate anaesthesia. This presumably reflects the fact that network activity is reduced under barbiturate anaesthesia, in agreement with previous experiments showing that the input resistance of cortical neurons during barbiturate anaesthesia is about half of that measured *in vitro*²².

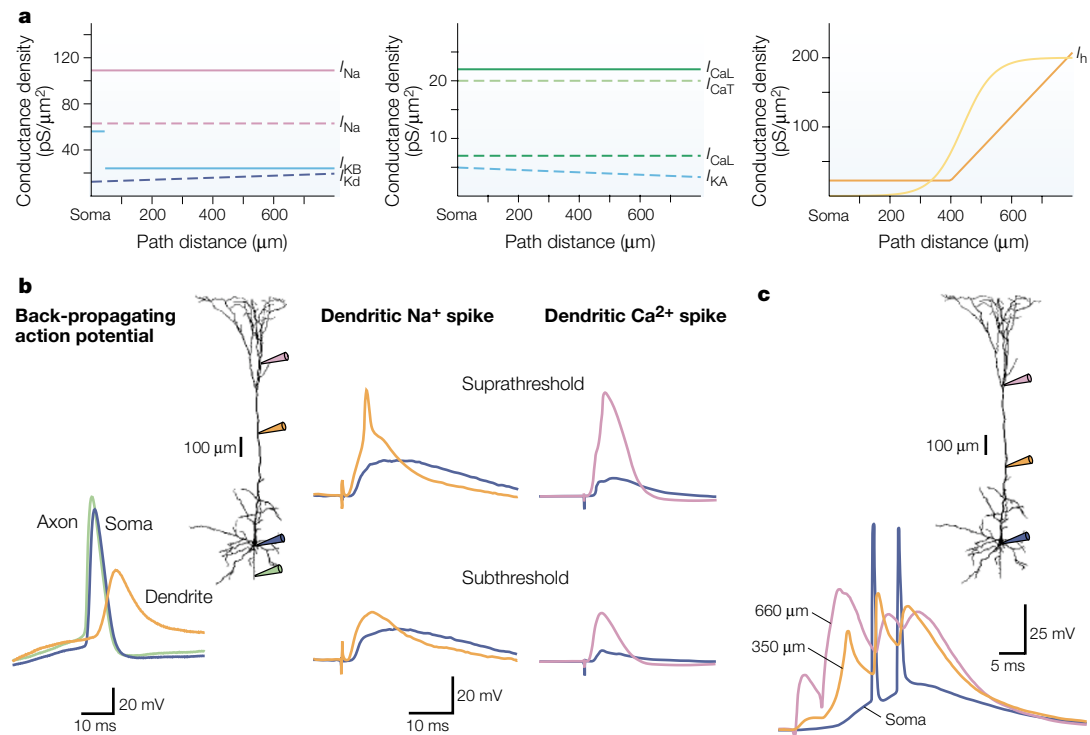


Figure 3 | **Dendritic excitability.** **a** | Somato-dendritic distribution of active channels in neocortical pyramidal neurons. Various voltage-dependent ion channels are present in neocortical dendrites, including the fast Na⁺ current I_{Na} (left³⁶), delayed-rectifier K⁺ current I_{Kd} (left⁴⁰), Ca²⁺-dependent K⁺ current I_{KB} (left⁴¹), A-type K⁺ current I_{KA} (middle⁴⁰), L-type (high-threshold) Ca²⁺ current I_{CaL} (middle⁴²), T-type (low-threshold) Ca²⁺ current I_{CaT} (middle⁴²) and hyperpolarization-activated current I_h (right; yellow⁴⁴ and orange⁴³). Results for young (dashed) and mature (solid) animals are shown. Unlike hippocampal CA1 neurons, the density of these conductances is fairly constant along the apical dendrites of neocortical pyramidal neurons, with the exception of I_h (see REF. 9). **b** | Active propagation of dendritic action potentials. Left: low-intensity stimuli applied at distal dendritic levels generate an action potential that is initiated in the axosomatic region (green and blue) and then back-propagates into the dendrite (orange). Right: simultaneous recordings from dendrites (orange, 400 μm from soma; pink, 920 μm from soma) and soma reveal both subthreshold and suprathreshold responses to distal synaptic stimulation. **c** | Forward propagation of dendritic spikes to the soma. Triple recording at different sites (inset) shows that dendritic spikes generated by coincidentally occurring excitatory postsynaptic potentials in distal dendrites can propagate to the soma and elicit somatic spikes. Panel **b** adapted, with permission, from REF. 10 © (2000) American Association for the Advancement of Science; Panel **c** adapted, with permission, from REF. 63 © (2002) American Association for the Advancement of Science.

From these measurements, we can estimate the relative contributions of excitatory and inhibitory conductances during high-conductance states. For a passive membrane, the average membrane potential ($\langle V_m \rangle$) at steady-state is given by:

$$\langle V_m \rangle = \frac{g_{leak} E_{leak} + \langle g_e \rangle E_e + \langle g_i \rangle E_i}{g_{leak} + \langle g_e \rangle + \langle g_i \rangle}$$

where $\langle \rangle$ denotes the time average, g_{leak} is the LEAK CONDUCTANCE, E_{leak} is the leak reversal, and g_e and g_i (and their respective reversal potentials E_e and E_i) are the time-dependent global excitatory and inhibitory conductances, respectively. Including in this equation results from *in vivo* measurements obtained under KX in the up state and after TTX^{17,23}, namely $\langle V_m \rangle = -65 \pm 2$ mV, $E_{leak} = -80 \pm 2$ mV, $E_e = 0$ mV, $E_i = -73.8 \pm 1.6$ mV and $R_{in}(TTX)/R_{in}(active) = 5.4 \pm 1.3$, yields the following ratios: $\langle g_e \rangle / g_{leak} = 0.73$ and $\langle g_i \rangle / g_{leak} = 3.67$.

According to these measurements, the ratio of the contributions of the average excitatory and inhibitory conductances, $\langle g_i \rangle / \langle g_e \rangle$, is about 5. Ratios between 4 and 5 are obtained in cells with reversed inhibition

(for example, recorded with chloride-filled electrodes¹⁷), or after brainstem stimulation (J. Pelletier & D.P., unpublished observations). Other *in vivo* experimental studies also concluded that inhibitory conductances are two- to sixfold larger than excitatory conductances during sensory responses²⁷⁻²⁹ or after thalamic stimulation³⁰ (but see REF. 31).

The data reviewed here indicate that when the EEG is desynchronized, neocortical neurons are in a 'high-conductance state' that is characterized by the following features: a large membrane conductance, which corresponds to a three- to fivefold decrease in input resistance; an average membrane potential (around -65 to -60 mV) that is significantly depolarized compared with the natural resting level (-70 to -80 mV); and large amplitude membrane potential fluctuations (σ_v of 2-6 mV), which are at least tenfold larger than those seen in the absence of network activity. In addition, the data indicate that these characteristics are attributable mostly to network activity, and that inhibitory conductances account for most of the large membrane conductance.

LEAK CONDUCTANCE
A constitutively active conductance, the reversal potential of which is called the leak reversal.

Dendritic excitability *in vitro*

A prerequisite for evaluating the impact of high-conductance states on neural processing in general, and mechanisms of dendritic integration in particular, is to characterize the electrophysiological properties of dendrites. The classic view of dendrites as passively conducting cable structures³² has changed greatly in the past few decades. A large body of experimental evidence has revealed that dendritic membranes are electrically excitable^{9,33,34} because they are endowed with a plethora of voltage-gated ion channels. *In vitro* recordings, and in particular whole-cell patch recordings (for example, REF 35), have not only shown the diversity of voltage-gated ion channels in dendrites, but have also mapped their distributions⁹ and revealed how their densities change during development³⁶.

Hippocampal pyramidal neurons have the best characterized dendrites⁹. However, the dendrites of neocortical neurons seem to possess the same types of voltage- and calcium-dependent ion channels^{33,37–39}. These include fast sodium currents³⁶, DELAYED-RECTIFIER POTASSIUM CURRENTS⁴⁰, calcium-dependent potassium currents⁴¹, A-TYPE POTASSIUM CURRENTS⁴⁰, high and low threshold calcium currents⁴², and hyperpolarization-activated currents⁴³ (FIG. 3a). However, the densities of sodium, potassium and calcium channels are lower in the dendrites of neocortical neurons than in hippocampal pyramidal neurons⁹. Moreover, the fairly constant density of these conductances along the apical dendrites of neocortical neurons contrasts with their strong location dependence in hippocampal neurons⁹. One exception to this is the hyperpolarization-activated current I_h , which has a lower density in the soma than in the apical tuft of neocortical neurons^{43,44} (FIG. 3a, right). Experimental data indicate that this non-uniform distribution of I_h might be responsible for a functional decoupling of the basal and apical dendrites⁴³. It also diminishes the effect of dendritic attenuation on the time course of the somatic excitatory postsynaptic potential (EPSP) and on TEMPORAL SUMMATION in neocortical neurons⁴⁵.

These active dendritic properties allow us to consider qualitatively new electrical behaviours and mechanisms of synaptic integration. The repertoire of possible interactions between voltage-dependent conductances and colocalized synapses ranges from the modulation of passive responses⁴⁶ to the subthreshold amplification of distal synaptic inputs at the soma^{43,45,47,48} (FIG. 3b, right bottom). However, it is the ability of dendrites to generate and propagate spikes^{49–53} that has the most important implications for synaptic integration.

Since they were first described in intracellular recordings of hippocampal neurons⁴⁹, two different classes of dendritic spikes have been distinguished. Action potentials generated in the axosomatic region, after current injection or synaptic stimulation, can actively propagate back into the dendritic tree^{10,54,55} (FIG. 3b, left), carrying retrograde signals from the soma to distal regions. The pairing of such active signals with local EPSPs in a narrow time window fosters the induction of either long-term potentiation (LTP) or long-term

depression (LTD), indicating that back-propagating dendritic spikes might be important in synaptic plasticity^{56,57}. Alternatively, the local integration of EPSPs can initiate dendritic sodium or calcium spikes (FIG. 3b, right top), which can propagate to the soma^{58–63} and eventually trigger somatic spikes (FIG. 3c). Forward-propagating dendritic spikes can boost the influence of synapses in distal dendrites on the soma, thereby circumventing the attenuation produced by the passive cable properties of dendrites^{8,18}.

Models of the high-conductance state

To investigate the integrative properties of neocortical neurons during high-conductance states, we must combine biophysical measurements of dendritic excitability with *in vivo* data on stochastic dynamics and high membrane conductances. To this end, several types of computational approach have been used. ‘Compartmental models’ integrate detailed three-dimensional morphological reconstructions of neurons. Most of the publicly available neuronal simulation environments, such as NEURON⁶⁴, allow users to incorporate morphological data and simulate the corresponding cable equations using a set of isopotential compartments. These compartmental models also integrate measurements of channel densities in the soma, dendrites and axon, as well as postsynaptic receptors for excitatory synapses (AMPA (α -amino-3-hydroxy-5-methyl-4-isoxazole propionic acid) and NMDA (*N*-methyl-D-aspartate) receptors) and inhibitory synapses (GABA_A (γ -aminobutyric acid subtype A) receptors). Various compartmental models have been proposed to model ‘synaptic noise’ in cortical neurons^{16,17,65} (BOX 1). These models simulate many individual synapses that are distributed in dendrites according to anatomical data¹. The random activity of these synapses can be adjusted to reproduce the high-conductance states observed *in vivo*. The model shown in BOX 1b was constrained by the *in vivo* data on KX up states discussed earlier. In addition, *in vivo* recordings of miniature synaptic events⁶⁶ were used to estimate quantal conductances¹⁷, which provide an important additional constraint. This model could reproduce all of the characteristics of high-conductance states under reasonable assumptions of release frequency (about 0.5–3 Hz and 4–8 Hz for excitatory and inhibitory synapses, respectively¹⁷).

Other approaches to modelling high-conductance states are either single-compartment models with multiple synaptic inputs^{67,68}, or single-compartment models containing ‘effective’ synaptic conductances⁶⁹ (BOX 1c). In the latter case, the synaptic conductances are modelled by stochastic processes that capture the statistical and spectral properties of the underlying synaptic inputs (see details in REF 69). All of these models can reproduce the characteristics of high-conductance states: a depolarized membrane potential (–65 mV); a three- to fivefold reduction in input resistance compared with the absence of network activity; large-amplitude voltage fluctuations ($\sigma_v \approx 4$ mV); and dominant inhibitory conductances ($g_i \approx 4g_e$). In addition, these models qualitatively capture the symmetric voltage distribution (BOX 1, middle

DELAYED RECTIFIER

K⁺ CHANNELS

Channels commonly found in axons, the conductance of which changes with a delay after a voltage step. They are important for the generation of action potential bursts, the regulation of pacemaker potentials and other functions.

A-TYPE K⁺ CHANNELS

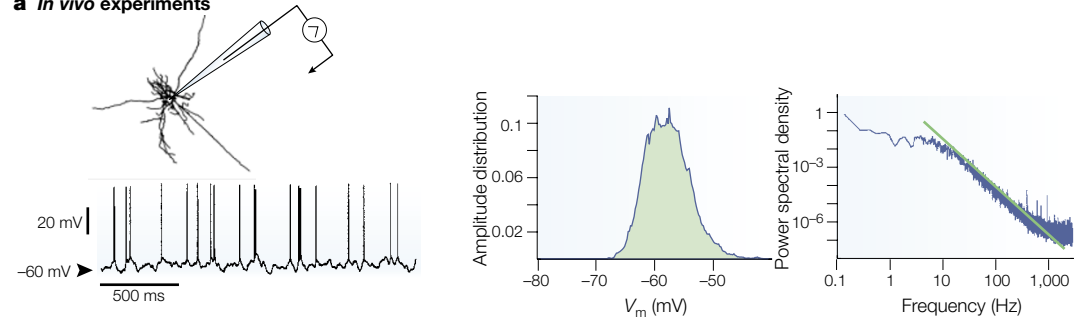
This type of channel activates and inactivates very rapidly in response to voltage changes, preventing neurons from responding to fast depolarizations.

TEMPORAL SUMMATION

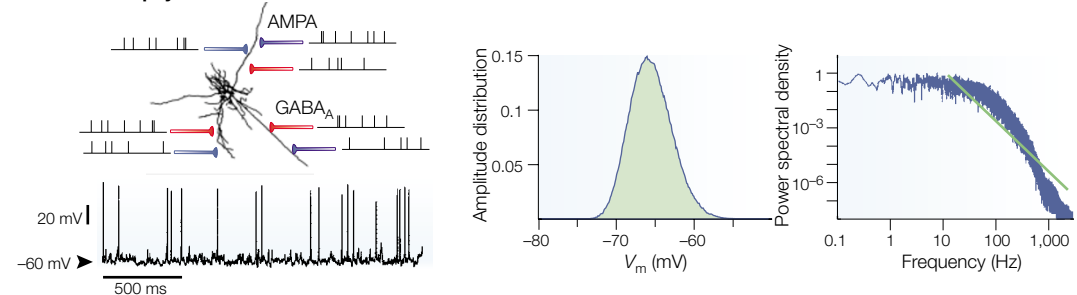
The way in which non-simultaneous synaptic events add in time. One of the basic elements of synaptic integration.

Box 1 | Synaptic noise

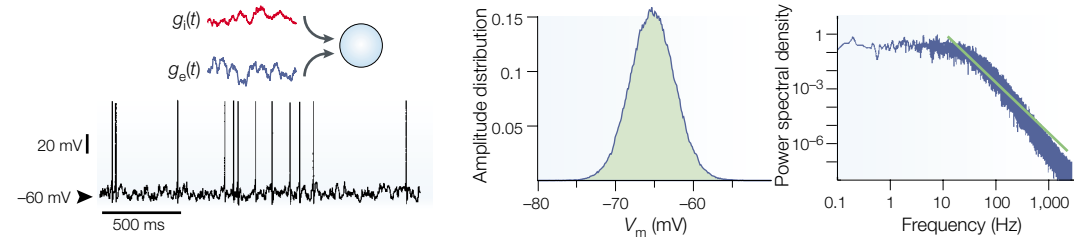
a *In vivo* experiments



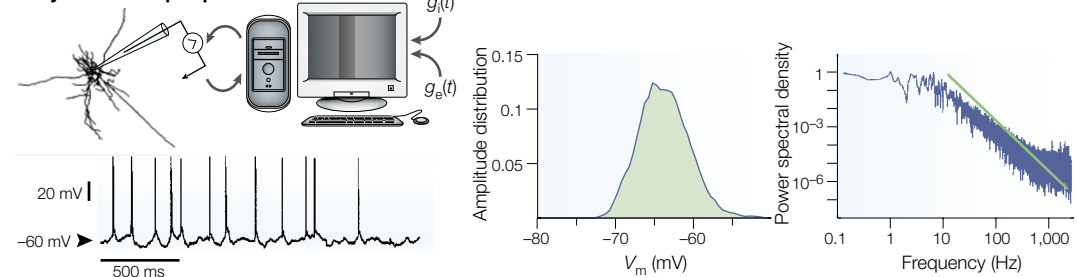
b Detailed biophysical models



c Point-conductance models



d Dynamic-clamp experiments



The term ‘synaptic noise’ is commonly used to describe the irregular subthreshold dynamics of the membrane potentials of neurons *in vivo*, which are caused by the discharge activity of a large number of presynaptic neurons. Despite carrying neuronal information, this activity seems to be nearly random, resulting in stochastic dynamics of the membrane potential, with statistical properties and a broadband POWER SPECTRUM that resemble those of COLOURED NOISE. Panel a shows synaptic ‘noise’ in neocortical neurons *in vivo* during activated periods with a desynchronized electroencephalogram (EEG). Panel b illustrates a detailed biophysical model of synaptic noise in a reconstructed layer VI pyramidal neuron, with Na⁺ and K⁺ channels in dendrites and soma. Randomly releasing excitatory ($n \approx 16,000$) and inhibitory ($n \approx 4,000$) synapses were modelled using AMPA (α -amino-3-hydroxy-5-methyl-4-isoxazole propionic acid) and GABA_A (γ -aminobutyric acid subtype A)-receptor kinetics¹⁷. Their distribution in soma and dendrites was based on ultrastructural measurements¹. Panel c shows a ‘point conductance’ model of synaptic noise; a single-compartment model with two global excitatory (g_e) and inhibitory (g_i) synaptic conductances, modelled by stochastic processes⁶⁹. Panel d shows the results of dynamic-clamp induction of synaptic noise in neocortical neurons *in vitro*. In each case, an example of the membrane potential time course (left), its amplitude distribution (middle) and its power spectral density (right; logarithmic scale) are shown. The power spectral densities were computed in the absence of spikes (hyperpolarized, or using passive models). In all cases, the distributions were approximately symmetric, and power spectral densities were broadband and behaved as a negative power of frequency ($1/f^k$, $k \approx 2.6$; green lines) at high frequencies (as expected for low-pass filtered noise). The data used for the analysis in d were kindly provided by M. Badoual and T. Bal.

POWER SPECTRUM

After analysing a waveform with a Fourier transform, its amplitude spectrum is the collection of amplitudes of the sinusoidal components that result from the analysis. The power spectrum is the square of the amplitude spectrum.

COLOURED NOISE

White noise is a signal that covers the entire range of component sound frequencies with equal intensity. In coloured noise, the signal covers a narrow band of frequencies.

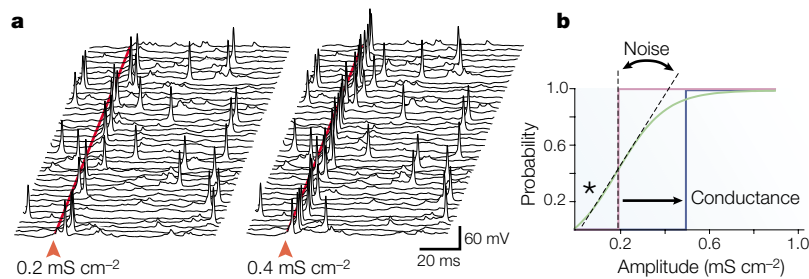


Figure 4 | Enhanced responsiveness during high-conductance states. **a** | Probabilistic dynamics of synaptically triggered action potentials in the presence of membrane potential fluctuations caused by spontaneous network activity. A simulated cortical pyramidal neuron in the high-conductance state (compartmental model shown in Box 1b) was stimulated by AMPA (α -amino-3-hydroxy-5-methyl-4-isoxazole propionic acid) synapses (arrow; two different stimulus intensities are shown; 40 trials each). Stimuli evoked action potentials with considerable trial-to-trial variability. **b** | Enhancement of responsiveness by voltage fluctuations. The response curve (probability of somatic spike response as a function of stimulus amplitude) is shown in three different states: quiescent (pink, absence of synaptic activity); static conductance (blue; additional constant conductance equivalent to the averaged conductance during high-conductance states); high-conductance state (green; synaptic activity as in **a**). The addition of a static conductance shifted the response curve towards a higher threshold (single arrow), whereas the ‘synaptic noise’ during high-conductance states changed the slope of the response curve (double arrow). Small inputs (for example, 0.1 mS cm^{-2} , asterisk) evoked a detectable response only in the latter case. Modified, with permission, from REF. 81 © (2000) American Physiological Society.

panels) and the broadband shape of the power spectrum of membrane potential fluctuations (BOX 1, right panels).

Network-level modelling studies have also investigated the genesis of self-sustained stochastic states resembling high-conductance states. A number of such studies were performed on INTEGRATE-AND-FIRE MODELS^{70–76} or using conductance-based spike-generating mechanisms^{77,78}. Most of these studies, however, did not use conductance-based synaptic interactions. As a result, it is impossible to compare the states obtained in these models with conductance measurements *in vivo*. So far, only one such study⁷⁸ has reported the genesis of self-sustained stochastic states with dominant inhibitory conductances, similar to *in vivo* measurements (see also REF. 79).

Consequences of high-conductance states

The impact of high-conductance states on the integrative properties of cortical neurons has been investigated using computational models. We summarize here the findings of several studies that predicted a number of ‘computational principles’ for high-conductance states, using multi- or single-compartment models.

A first consequence is that the responsiveness of cortical neurons is markedly different in the presence of fluctuating background synaptic activity. Owing to the presence of membrane potential fluctuations, neurons respond stochastically to a given stimulus. In fact, their behaviour is best described by probability functions. An example of such a probabilistic response is given in FIG. 4a. Using probabilities to quantify synaptic efficacy (defined here as the probability that a given synaptic input specifically evokes an action potential at the soma; for another measure, see REF. 80) shows the contrasting effects of conductance and membrane potential fluctuations on the responsiveness of cortical

neurons. FIGURE 4b contrasts the same compartmental model in three states: a ‘quiescent’ state (pink), in which membrane properties were adjusted to *in vitro* recordings; a high-conductance state (green), which simulates stochastic synaptic inputs as in BOX 1b; and an equivalent static conductance (blue), in which the sole conductance factor of synaptic activity was retained and incorporated through an additional leak conductance. Cortical cells *in vitro* behave like binary devices, showing a sharp threshold as a function of stimulus intensity (‘all-or-none’ response function) (FIG. 4b, pink). The introduction of a static high conductance alone results in a decreased responsiveness (FIG. 4b, blue), consistent with a pure shunting effect. By contrast, voltage fluctuations (‘synaptic noise’) significantly change the response curve (FIG. 4b, green; see change in slope). Remarkably, this curve shows that there is a small response probability for inputs that were subthreshold in all other cases, showing an enhanced responsiveness to low-amplitude inputs⁸¹ (FIG. 4b, asterisk). This phenomenon is comparable to STOCHASTIC RESONANCE, which is found in many non-linear systems⁸², in simple neuronal models^{83,84}, and in experimental⁸⁵ and theoretical⁸⁶ studies of central neurons. The situation described here is different, as synaptic noise also decreases responsiveness through the increased conductance. The enhancement of responsiveness can also be seen at the level of dendrites, where synaptic noise can boost the ability of stimuli to initiate dendritic spikes¹⁸ (see later in text). Therefore, a first prediction of modelling studies is that voltage fluctuations at levels comparable to *in vivo* measurements should significantly alter the responsiveness of cortical neurons.

A second main consequence of high-conductance states is that they greatly affect the efficacies of synaptic inputs at different dendritic sites. In passive dendrites, the high-conductance state increases voltage attenuation and reduces the time constant. These effects can be deduced from CABLE THEORY⁸⁷ and were proposed in early theoretical studies^{14,15}. The impact of high-conductance states on the attenuation of EPSPs is shown in FIG. 5a. Excitatory synaptic inputs were simulated at different dendritic sites in a compartmental model of a cortical pyramidal neuron, and the EPSP peak was represented against distance and stimulus amplitude. In quiescent conditions (FIG. 5a, left), EPSPs are differentially filtered as a function of their position. Addition of the static high conductance (FIG. 5a, middle) leads to much stronger attenuation, with distal inputs having negligible impact at the level of the soma for distances of a few hundred micrometres.

So, a high conductance severely reduces the likelihood that distal inputs will influence somatic spiking. One possible solution to this problem is the presence of voltage-dependent conductances, which can lead to different normalizations of synaptic efficacy^{9,43,45,46,48}. Another possible solution is to rescale synaptic conductances in proportion to the distance from the soma, so that all synapses evoke roughly equivalent somatic EPSPs, as observed in hippocampal pyramidal neurons⁸⁸. However, patch-clamp recordings indicate that such re-scaling does not occur in neocortical neurons⁸.

INTEGRATE-AND-FIRE MODEL
The simplest model of a spiking neuron that takes into account the dynamics of the synaptic inputs.

STOCHASTIC RESONANCE
The facilitated or optimized response of a non-linear dynamical system to stimuli in the presence of non-vanishing noise, usually expressed as a peak of the signal-to-noise ratio.

CABLE THEORY
Mathematical description of the purely passive spread of electrical current in a nerve fibre. It is conceptually similar to the theory that is needed to understand the properties of long cables.

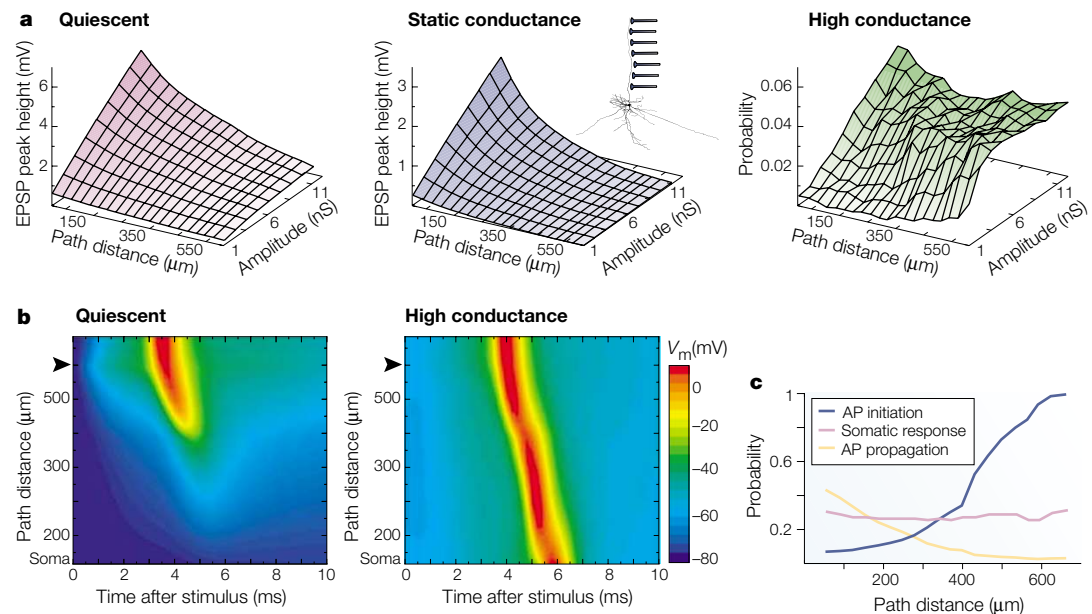


Figure 5 | Equalization of synaptic efficacies during high-conductance states. **a** | Comparison of synaptic efficacies during quiescent and high-conductance states. AMPA (α -amino-3-hydroxy-5-methyl-4-isoxazole propionic acid) receptor-mediated synapses were simulated at different sites (inset) and the response was represented against path distance from the soma and stimulus amplitude. In quiescent conditions (left), distal inputs are moderately attenuated, as predicted by cable theory. With static high conductance (middle), the attenuation was increased several-fold, leading to almost complete filtering of distal synaptic inputs. During high-conductance states (right), the efficacy of synaptic inputs (defined as the total probability that a synaptic stimulus evokes a somatic spike) was weakly dependent on the dendritic location of the synapse. EPSP, excitatory postsynaptic potential. **b** | Enhancement of action potential initiation and propagation by synaptic activity. A forward-propagating dendritic action potential was evoked in a distal dendrite by an AMPA receptor-mediated excitatory postsynaptic potential (arrow). In quiescent conditions (left), this action potential propagated for only 100–200 μm , even for high-amplitude stimuli (9.6 nS shown). In high-conductance states (right), dendritic action potentials could propagate up to the soma, even for small stimulus amplitudes (2.4 nS shown). **c** | The location independence of synaptic efficacy can be explained by the probabilities of dendritic action potential (AP) initiation and propagation. The probability that a synaptic stimulus will initiate a dendritic spike (blue) and the probability that a dendritic spike evoked by the stimulus will propagate to the soma and elicit a somatic spike (yellow) are represented as functions of the distance of the stimulating synaptic input. Synaptic efficacy, which is the product of these two probabilities (pink; values multiplied by 10), shows nearly location-independent behaviour. Modified, with permission, from REF. 18 © (2003) Society for Neuroscience.

Another solution to this dilemma might arise from the dynamics of dendritic integration during high-conductance states^{18,89}. Theoretical studies predict that synaptic inputs ending at different dendritic sites have roughly equivalent efficacies during these states (FIG. 5a, right). This remarkable result can be understood from two properties. First, the initiation of action potentials in dendrites is facilitated by voltage fluctuations¹⁸, through mechanisms similar to that underlying enhanced responsiveness (FIG. 4b). Second, dendritic action potentials might show facilitated propagation during high-conductance states (propagation is ‘facilitated’ in the sense that in stochastic states, all dendritic spikes have some probability of propagating up to the soma, whereas a significant fraction of them, especially in distal sites, fail in quiescent conditions). These effects are shown in FIG. 5b; in quiescent states, dendritic action potentials are highly sensitive to variations in local electrophysiological and morphological characteristics, and sometimes fail to propagate reliably (FIG. 5b, left), whereas in high-conductance states even small stimuli can elicit dendritic spikes, which reliably propagate up to the soma (FIG. 5b, right). The location independence can be understood

from these probabilities of dendritic spike initiation and propagation, which show opposite location dependence; the probability of dendritic spike initiation is larger for distal sites (FIG. 5c, blue) because of the higher local input resistance of thinner dendrites. The probability for spike propagation to the soma shows inverse dependence on distance (FIG. 5c, yellow), because distally initiated spikes have more chances to be ‘intercepted’ by inhibitory synaptic events or dendritic spikes along the way. Remarkably, these dependences compensate, such that synaptic efficacy, which is the product of these two probabilities, is approximately location independent (FIG. 5c, pink). These results indicate that, owing to interactions between synaptic noise, voltage-dependent channels and dendritic morphology, the efficacy of synaptic inputs has a reduced location dependence during high-conductance states.

A third effect of high-conductance states is on temporal processing. The reduction of the space constant in states of high conductance is accompanied by a marked reduction in the MEMBRANE TIME CONSTANT^{16,17}, which is apparent in experimental data, for example in the faster response to injected current (FIG. 2c, averaged traces).

MEMBRANE TIME CONSTANT
A quantity that depends on the capacitance and resistance of the cell membrane, and which sets a timescale for changes in voltage. A small time constant means that the membrane potential can change rapidly.

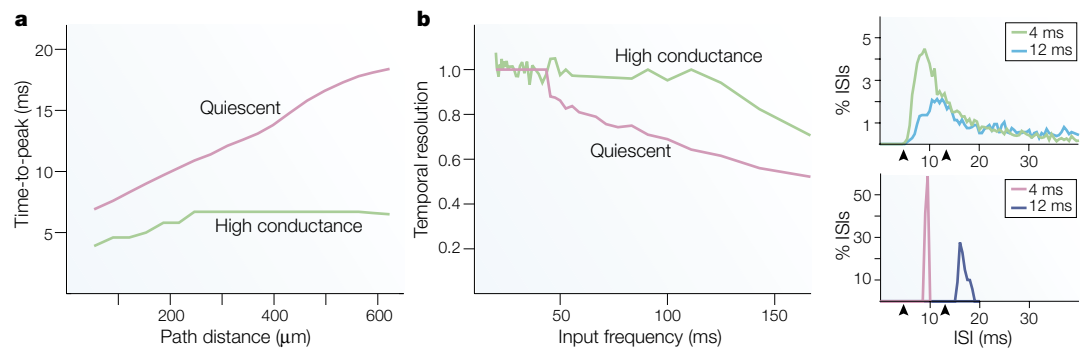


Figure 6 | **Sharper temporal resolution during high-conductance states.** **a** | Location-dependence of the timing of excitatory postsynaptic potentials (EPSPs). A similar stimulation model as in Fig. 5a was used, except that the time-to-peak of averaged synaptic responses is represented against distance to soma. In quiescent conditions (pink), the time-to-peak of EPSPs increased approximately linearly with distance from soma. This location dependence was markedly reduced in the high-conductance state (green). **b** | Enhanced temporal resolution of synaptic inputs during the high-conductance state. AMPA (α -amino-3-hydroxy-5-methyl-4-isoxazole propionic acid) receptor-mediated synaptic inputs were delivered at different frequencies (model used is identical to Box 1c). The temporal resolution was quantified by computing the ratio between the stimulus interval and the mode of the corresponding interspike interval histogram. In quiescent conditions (left panel, pink), the model could respond reliably up to a stimulus frequency of about 50 Hz. In high-conductance states (left panel, green), the frequency following was reliable up to much higher frequencies (beyond 100 Hz). The right panels show examples of interspike interval (ISI) histograms for stimulation at 4 ms and 12 ms interstimulus intervals, for the quiescent (top) and high-conductance (bottom) states. Panel **a** modified, with permission, from REF. 18 © (2003) Society for Neuroscience; Panel **b** modified, with permission, from REF. 91 © (2003) Elsevier Science.

As proposed about 30 years ago¹⁴, this reduced time constant should favour finer temporal discrimination of distant synaptic inputs^{15,16,18}. In active dendritic structures, small membrane time constants also promote fast-propagating action potentials, resulting in a reduced location-dependence of EPSP timing¹⁸ (FIG. 6a). This might facilitate the association of distant inputs at a higher temporal resolution. Consistent with this, a relationship was found between the high-conductance state and the typical irregular firing of neocortical neurons^{67,90}. Perhaps the most striking consequence, however, is that neurons can resolve higher frequency inputs in high-conductance states than when quiescent⁹¹, as illustrated in FIG. 6b. Models therefore predict that cortical neurons in high-conductance states can efficiently and rapidly track synaptic inputs⁷⁹.

Other computational advantages of high-conductance states have been noted in modelling studies. First, because both excitatory and inhibitory conductances are large during high-conductance states, slight variations of either excitation or inhibition are effective in modifying spiking probability. As a consequence, neurons can reliably detect faint changes in temporal correlation of the random activity of their inputs^{92,93}. This type of response is interesting, because it is not accompanied by average changes in membrane potential or membrane conductance. In fact, neurons respond to the variance of the conductances, only causing instantaneous changes in the membrane potential (which cannot be modelled by rate-based neuron models). This type of response, which was also found experimentally⁹⁴⁻⁹⁶, deserves further study.

Second, synaptic activity has an important impact on the operating mode (coincidence detection versus firing-rate integration) of cortical neurons⁹⁷; neurons can use different coding strategies in parallel⁹⁸⁻¹⁰⁰

or even continuously switch between them. This possibility is in agreement with modelling studies based on integrate-and-fire neurons¹⁰¹, and with the linear relationship found between the degree of synaptic synchrony and cellular responses¹⁰².

Finally, models predict that enhanced voltage attenuation during high-conductance states should favour the electrical isolation of dendritic segments with respect to each other. This would result in a dendritic tree in which subregions could independently integrate synaptic inputs and perform relatively independent computations. This concept is similar to the ‘dendritic subunits’ postulated in previous theoretical studies¹⁰³. Such a functional parcellation could increase the computational power of dendritic trees. Recently, a similar compartmentalized (in the sense of local processing) and parallelized (in the sense of independently processing subunits) dendritic dynamic was proposed on the basis of *in vitro* experimental observations of active signalling in individual terminal dendritic branches⁶². It was also predicted by modelling studies¹⁸ (FIG. 5b), which indicates that dendritic spikes might not only carry the results of local dendritic computations, but also serve as a channel through which distal dendritic subunits send their information to the soma, therefore participating in shaping the cellular response.

So, models predict that high-conductance states confer a number of advantageous properties on neocortical neurons, the main one being fine discrimination of inputs, not only in the amplitude domain (enhanced responsiveness), but also in spatial and temporal domains. The drawback of this integrative mode is that the system is inherently stochastic, producing a response only with some probability. However, this property should be compensated for by populations of neurons processing information in parallel¹⁰⁴.

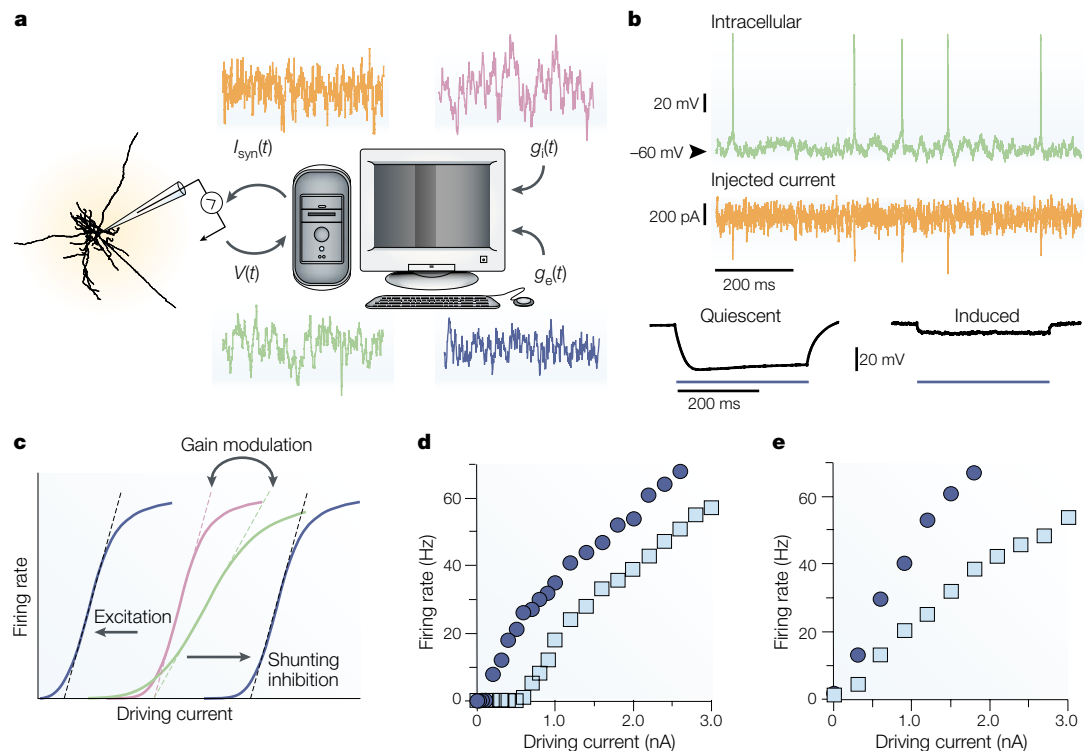


Figure 7 | **Dynamic-clamp experiments *in vitro* reproduce *in vivo* high-conductance states.** **a** | Dynamic-clamp protocol. The membrane potential $V(t)$, obtained by an intracellular recording (green), is combined with computational models of a stochastic conductance time course (where $g_e(t)$ and $g_i(t)$ are the excitatory and inhibitory conductances, respectively). The resulting effective synaptic current (orange) $i_{syn}(t) = g_e(t)(E_e - V(t)) + g_i(t)(E_i - V(t))$ (where E_e and E_i are the reversal potentials for the excitatory and inhibitory conductances, respectively) is injected into the cell (current-clamp mode), inducing stochastic neuronal activity (same model as in Box 1c). **b** | Recreation of high-conductance states in neocortical neurons *in vitro*. Top: the stochastic activity induced by the noisy injected current (orange) is characterized by a depolarized and fluctuating membrane potential as well as irregular discharges (green; see also Box 1d). Bottom: the membrane shows a markedly reduced input resistance (induced) resulting in a diminished response to injected currents (blue bars; compare with Fig. 2c). **c** | Contrasting effects of conductance and noise. The sigmoidal response curve in control conditions (pink) can be shifted to lower or larger stimulus amplitudes (stimuli were driving currents in this case) by changes in static conductances (blue; left- or right-shifts are produced by increases of excitatory or inhibitory conductances, respectively). By contrast, changing synaptic noise at equivalent conductance levels modified the slope of the response curve (green), which can be described as 'gain modulation'. **d** | Dynamic-clamp evidence for the effect of static conductances on the working point of the response curve (SHUNTING INHIBITION; blue circles: control response curve for excitatory and inhibitory without additional conductance; blue squares: response with additional static conductance of 32 nS). **e** | Dynamic-clamp evidence for gain modulation by synaptic noise. In this case, the slope of the response curve was altered compared with control conditions (blue circles) by a threefold increase of the release rates at excitatory and inhibitory synaptic terminals (blue squares). The latter modulation increases both the noise amplitude and the amount of shunting. Panel **b** reproduced, with permission, from REF. 69 © (2001) Elsevier Science; Panels **c–e** modified, with permission, from REF. 109 © (2002) Elsevier Science.

Dynamic-clamp experiments

To evaluate the impact of high-conductance states on real neurons, techniques are needed to recreate these states in simple preparations. Some studies have investigated the effects of injecting noisy current waveforms *in vitro*^{105,106}, but in this case, neurons are in a low-conductance state. To simulate the conditions of an intact network, conductances must be injected into the cell. This is possible through the dynamic-clamp technique (FIG. 7a), which was introduced a decade ago^{107,108} and is equivalent to adding a 'virtual' conductance in the membrane of a real neuron. Implementing this system in cortical slices^{69,109–112} yields a state of stochastic activity similar to that seen *in vivo*⁶⁹ (BOX 1d), with a depolarized and fluctuating membrane potential (FIG. 7b, top and bottom left), irregular firing and a markedly reduced input resistance (FIG. 7b, bottom right; compare with FIG. 1c).

SHUNTING INHIBITION

A phenomenon whereby membrane depolarization that is induced by a given current is attenuated because of an enhanced membrane conductance.

Dynamic-clamp combines all the approaches described earlier in this review. First, *in vivo* electrophysiology provides qualitative and quantitative information about the voltage and conductance dynamics in states of intense cortical network activity. Second, computational modelling provides models of the conductance fluctuations during high-conductance states (BOX 1c,d). Third, *in vitro* electrophysiology is used with the dynamic-clamp protocol to 'recreate' the characteristics of high-conductance states as measured *in vivo*⁶⁹. The limitation of this approach is that conductances can only be injected at the site of electrode impalement (usually the soma), whereas real synaptic inputs are distributed in dendrites. Nevertheless, the dynamic-clamp captures the interplay of currents in the proximal region of the cell, and the benefit of this approach is that one can take advantage of the fine control over synaptic

inputs achievable *in vitro*, while having cellular characteristics comparable to *in vivo* recordings. This reproduction of specific *in vivo* states provides a powerful way to test theoretical predictions that could hardly be addressed *in vivo*.

The effect of high-conductance states on responsiveness can be tested by dynamic-clamp experiments. In agreement with model predictions, injection of stochastic conductances in cortical neurons *in vitro* profoundly altered their responsiveness, or equivalently, neuronal gain^{109–112}. The response function of the neuron usually takes the form of a sigmoidal function of stimulus amplitude (FIG. 7c, pink), and two aspects of this function can be modulated: its sensitivity, defined by the slope (‘gain’) of the response curve (FIG. 7c, green), and its working point, defined by the position of the response curve (FIG. 7c, blue). Both types of gain modulation arise from different manipulations of the synaptic conductances, which was proposed as a fundamental principle of neuronal computation¹¹³. In agreement with modelling predictions^{81,91} and cable theory, these experiments revealed that variations in the static (time-averaged or ‘leak’) conductance component cause shifts in the working point (subtractive modulation). Here, an increasing excitatory conductance shifts the response curve to lower stimulation amplitudes (FIG. 7c,d), whereas an increasing inhibitory conductance has the opposite effect^{109,111} (shunting inhibition). Divisive gain modulation, on the other hand, consists of a change in the slope of the response curve (FIG. 7c, green) and, therefore, a change in the sensitivity. This effect was found for balanced variations in excitatory and inhibitory firing rates¹⁰⁹ (FIG. 7d), or by varying directly the stochastic component of the synaptic conductances without changing its mean^{110,112}, in agreement with model predictions⁸¹.

So, dynamic-clamp experiments support the idea that stochastic conductances stemming from intense network activity are responsible for a general enhancement of responsiveness. Moreover, the amount of conductance and membrane potential fluctuations identified *in vivo* drastically alter the responsiveness of cortical neurons. These studies agree with previous observations that stimulation of the ascending activating systems leads to enhanced responsiveness^{114,115}, and that cortical neurons are more responsive during attentive states¹¹⁶.

Conclusions

Experiments and models indicate that the intense synaptic activity seen *in vivo* is not detrimental, but can confer advantageous computational properties on neocortical neurons. We now summarize these computational principles, possible ways to test them experimentally and perspectives for future work.

Enhanced responsiveness and gain modulation. The prediction⁸¹ that conductance noise enhances the responsiveness of cortical cells to low-amplitude inputs while decreasing responsiveness to large-amplitude inputs (FIG. 4) was confirmed experimentally^{85,109–112}. These effects were described collectively as ‘gain modulation’

by synaptic inputs. Because unitary inputs between pyramidal neurons have a small conductance¹¹⁷, the main effect of conductance noise is probably to enhance communication between single pyramidal neurons and to reduce the impact of highly synchronized inputs.

The high-conductance state and associated responsiveness should be characterized for other cell types, such as bursting neurons, and for other behavioural states, such as sleep (see REF. 7 for conductance measurements during slow-wave and paradoxical sleep), different levels of neuromodulators, or different attentional or arousal levels. In particular, the proposed link between enhanced responsiveness and attentional mechanisms⁸¹ would be worth investigating using intracellular experiments.

Equalization of synaptic efficacies. During high-conductance states, the complex interplay between conductance noise, voltage-dependent currents and dendritic action potentials can result in an equalization of the efficacy of individual synapses (FIG. 5). In parallel to this equalization, inputs are integrated more locally in dendrites, although their individual impact shows little dependence on the morphological details of the dendritic tree. These predictions¹⁸ could be tested by performing dual dendrite and soma recordings, together with a double dynamic-clamp injection of conductance noise.

To characterize further the integrative properties during high-conductance states, the following issues should be investigated computationally or using a combination of dynamic-clamp with dendritic recordings: the dependence of synaptic efficacy on morphology, and how combinations of inputs influence the soma as a function of their respective locations in dendrites and delays of activation.

Increased temporal resolution. Modelling studies^{14–18} have predicted that neurons in high-conductance states should have sharper temporal processing capabilities. First, there is reduced site-dependence of the timing of somatic responses (FIG. 6a). Second, neuronal responses have an augmented capacity to follow high-frequency synaptic stimulation (FIG. 6b). Third, neurons can detect rapid (~2 ms) changes of temporal correlation among thousands of input sources⁹³. No direct experimental tests of these predictions are available so far, although straightforward dynamic-clamp experiments could address this issue (FIG. 6b).

Models further indicate that the variance of conductances reflects the correlation in presynaptic activity⁶⁹, and changes in temporal correlation (or conductance variance) have powerful effects on neuronal responses^{67,92,93}. However, there is currently no method to estimate conductance variances from experiments (but see REF. 118). Theoretical studies should therefore investigate how to ‘deconvolute’ the synaptic noise that is recorded experimentally, perhaps providing methods to estimate conductance variances and the degree of temporal correlation in presynaptic activity.

Probabilistic and irregular behaviour. The dynamics of neurons in high-conductance states are inherently stochastic and responses show considerable variability (FIG. 4a), as typically found *in vivo*^{119,120}. The appropriate measure for such responses is to compute probabilities, as routinely done *in vivo* through the use of post-stimulus time histograms. This variability should disappear at the population level if responses from many neurons are pooled together¹⁰⁴. Therefore, neuronal populations should produce sensitive, precise and discriminative responses during high-conductance states.

Future theoretical studies should explore how cellular properties translate into global properties at the level of large populations of neurons. For example, the finding that low-amplitude excitatory inputs have

a small — but non-zero — probability of evoking spikes in high-conductance states^{81,109–112} might have interesting consequences at the network level. If the divergence of connectivity is larger than the inverse of the response probability to unitary inputs ($1/P_u$), then one spike in a given neuron will generally be followed by at least one spike in another neuron in the network, perhaps resulting in special collective properties.

Investigations of this type are needed to explore the processing capabilities of networks in high-conductance states, with the ultimate goal of understanding the computational operations of the intact and functioning neocortex. Meeting this challenge will necessarily require a continuous and tight association of *in vivo* and *in vitro* experiments with computational models.

- deFelipe, J. & Fariñas, I. The pyramidal neuron of the cerebral cortex: morphological and chemical characteristics of the synaptic inputs. *Prog. Neurobiol.* **39**, 563–607 (1992).
- Braitenberg, V. & Schüz, A. *Cortex: Statistics and Geometry of Neuronal Connectivity* 2nd edn (Springer, Berlin, 1998).
- Evarts, E. V. Temporal patterns of discharge of pyramidal tract neurons during sleep and waking in the monkey. *J. Neurophysiol.* **27**, 152–171 (1964).
- Steriade, M. & McCarley, R. W. *Brainstem Control of Wakefulness and Sleep* (Plenum, New York, 1990).
- Matsumura, M., Cope, T. & Fetzi, E. E. Sustained excitatory synaptic input to motor cortex neurons in awake animals revealed by intracellular recording of membrane potentials. *Exp. Brain Res.* **70**, 463–469 (1988).
- Baranyi, A., Szente, M. B. & Woody, C. D. Electrophysiological characterization of different types of neurons recorded *in vivo* in the motor cortex of the cat. II. Membrane parameters, action potentials, current-induced voltage responses and electrotonic structures. *J. Neurophysiol.* **69**, 1865–1879 (1993).
- Steriade, M., Timofeev, I. & Grenier, F. Natural waking and sleep states: a view from inside neocortical neurons. *J. Neurophysiol.* **85**, 1969–1985 (2001).
First intracellular recordings during different behavioural states. The same neurons are shown to experience consistent changes of membrane parameters across periods of waking, slow-wave sleep and rapid eye movement sleep.
- Williams, S. R. & Stuart, G. J. Role of dendritic synapse location in the control of action potential output. *Trends Neurosci.* **26**, 147–154 (2003).
- Migliore, M. & Shepherd, G. M. Emerging rules for the distributions of active dendritic conductances. *Nature Rev. Neurosci.* **3**, 362–370 (2002).
- Häusser, M., Spruston, N. & Stuart, G. J. Diversity and dynamics of dendritic signaling. *Science* **290**, 739–744 (2000).
- Cash, S. & Yuste, R. Linear summation of excitatory inputs by CA1 pyramidal neurons. *Neuron* **22**, 383–394 (1999).
- Pouille, F. & Scanziani, M. Enforcement of temporal fidelity in pyramidal cells by somatic feed-forward inhibition. *Science* **293**, 1159–1163 (2001).
- Stuart, G. J. & Häusser, M. Dendritic coincidence detection of EPSPs and action potentials. *Nature Neurosci.* **4**, 63–71 (2001).
Experimental demonstration that EPSPs interact non-linearly with dendritic spikes, resulting in a coincidence detection mechanism.
- Barrett, J. N. Motoneuron dendrites: role in synaptic integration. *Fed. Proc.* **34**, 1398–1407 (1975).
Theoretical paper investigating synaptic integration where the possible consequences of high-conductance states on integrative properties were mentioned for the first time.
- Holmes, W. R. & Woody, C. D. Effects of uniform and non-uniform synaptic 'activation-distributions' on the cable properties of modeled cortical pyramidal neurons. *Brain Res.* **505**, 12–22 (1989).
- Bernander, O., Douglas, R. J., Martin, K. A. & Koch, C. Synaptic background activity influences spatiotemporal integration in single pyramidal cells. *Proc. Natl Acad. Sci. USA* **88**, 11569–11573 (1991).
- Destexhe, A. & Paré, D. Impact of network activity on the integrative properties of neocortical pyramidal neurons *in vivo*. *J. Neurophysiol.* **81**, 1531–1547 (1999).
- Rudolph, M. & Destexhe, A. A fast-conducting, stochastic integrative mode for neocortical neurons *in vivo*. *J. Neurosci.* **23**, 2466–2476 (2003).
Theoretical paper showing that cortical neurons in high-conductance states might obey drastically different rules of dendritic integration compared with low-conductance states.
- Brock, L. G., Coombs, J. S. & Eccles, J. C. The recording of potential from motoneurons with an intracellular electrode. *J. Physiol. (Lond.)* **117**, 431–460 (1952).
- Woody, C. D. & Gruen, E. Characterization of electrophysiological properties of intracellularly recorded neurons in the neocortex of awake cats: a comparison of the response to injected current in spike overshoot and undershoot neurons. *Brain Res.* **158**, 343–357 (1978).
First intracellular study reporting that cortical neurons are in a high-conductance state in awake animals.
- Berthier, N. & Woody, C. D. *In vivo* properties of neurons of the precuneate cortex of cats. *Brain Res. Bull.* **21**, 385–393 (1988).
- Bindman, L. J., Meyer, T. & Prince, C. A. Comparison of the electrical properties of neocortical neurons in slices *in vitro* and in the anesthetized rat. *Exp. Brain Res.* **69**, 489–496 (1988).
- Paré, D., Shink, E., Gaudreau, H., Destexhe, A. & Lang, E. J. Impact of spontaneous synaptic activity on the resting properties of cat neocortical neurons *in vivo*. *J. Neurophysiol.* **79**, 1450–1460 (1998).
First characterization of synaptic background activity *in vivo*; the first study in which the same neurons were compared between active network states and after total suppression of network activity.
- Contreras, D., Timofeev, I. & Steriade, M. Mechanisms of long lasting hyperpolarizations underlying slow sleep oscillations in cat corticothalamic networks. *J. Physiol. (Lond.)* **494**, 251–264 (1996).
- Steriade, M., Amzica, F. & Nuñez, A. Cholinergic and noradrenergic modulation of the slow (-0.3 Hz) oscillation in neocortical cells. *J. Neurophysiol.* **70**, 1384–1400 (1993).
- Kasanez, F., Riquelme, L. A. & Murer, M. G. Disruption of the two-state membrane potential of striatal neurons during cortical desynchronization in anaesthetized rats. *J. Physiol. (Lond.)* **543**, 577–589 (2002).
- Borg-Graham, L. J., Monier, C. & Frégnac Y. Visual input evokes transient and strong shunting inhibition in visual cortical neurons. *Nature* **393**, 369–373 (1998).
- Hirsch, J. A., Alonso, J. M., Clay Reid, R. & Martinez, L. M. Synaptic integration in striate cortical simple cells. *J. Neurosci.* **18**, 9517–9528 (1998).
- Anderson, J. S., Carandini, M. & Ferster, D. Orientation tuning of input conductance, excitation and inhibition in cat primary visual cortex. *J. Neurophysiol.* **84**, 909–926 (2000).
- Contreras, D., Destexhe, A. & Steriade, M. Intracellular and computational characterization of the intracortical inhibitory control of synchronized thalamic inputs *in vivo*. *J. Neurophysiol.* **78**, 335–350 (1997).
- Shu, Y., Hasenstaub, A. & McCormick, D. A. Turning on and off recurrent balanced cortical activity. *Nature* **423**, 288–293 (2003).
- Rall, W. Electrophysiology of a dendritic neuron model. *Biophys. J.* **2**, 145–167 (1962).
- Linás, R. R. Electroresponsive properties of dendrites in central neurons. *Adv. Neural.* **12**, 1–13 (1975).
A visionary review paper on the importance of active dendritic properties in central neurons.
- Segev, I. & Rall, W. Excitable dendrites and spines: earlier theoretical insights elucidate recent direct observations. *Trends Neurosci.* **21**, 453–460 (1998).
- Williams, S. R. & Stuart, G. J. Action potential backpropagation and somato-dendritic distribution of ion channels in thalamocortical neurons. *J. Neurosci.* **20**, 1307–1317 (2000).
- Huguenard, J. R., Hamill, O. P. & Prince, D. A. Developmental changes in Na⁺ conductances in rat neocortical neurons: appearance of a slowly inactivating component. *J. Neurophysiol.* **59**, 778–795 (1988).
- Johnston, D., Magee, J. C., Colbert, C. M. & Christie, B. R. Active properties of neuronal dendrites. *Annu. Rev. Neurosci.* **19**, 165–186 (1996).
- Yuste, R. & Tank, D. W. Dendritic integration in mammalian neurons, a century after Cajal. *Neuron* **16**, 701–716 (1996).
- Stuart, G. J., Spruston, N. & Häusser, M. (eds) *Dendrites* (MIT Press, Cambridge, Massachusetts, 2000).
- Bekkers, J. M. Properties of voltage-gated potassium currents in nucleated patches from large layer 5 cortical pyramidal neurons of the rat. *J. Physiol. (Lond.)* **525**, 593–609 (2000).
- Kang, J., Huguenard, J. R. & Prince, D. A. Development of BK channels in neocortical pyramidal neurons. *J. Neurophysiol.* **76**, 188–198 (1996).
- Hamill, O. P., Huguenard, J. R. & Prince, D. A. Patch-clamp studies of voltage gated currents in identified neurons of the rat cerebral cortex. *Cereb. Cortex* **1**, 48–61 (1991).
- Berger, T., Larkum, M. E. & Lüscher, H. R. High I_h channel density in the distal apical dendrite of layer V pyramidal cells increases bidirectional attenuation of EPSPs. *J. Neurophysiol.* **85**, 855–868 (2001).
- Stuart, G. & Spruston, N. Determinants of voltage attenuation in neocortical pyramidal neuron dendrites. *J. Neurosci.* **18**, 3501–3510 (1998).
- Williams, S. R. & Stuart, G. J. Site independence of EPSP time course is mediated by dendritic I_h in neocortical pyramidal neurons. *J. Neurophysiol.* **83**, 3177–3182 (2000).
- Koch, C. Cable theory in neurons, with active, linearized membranes. *Biol. Cybern.* **50**, 15–33 (1984).
- Crill, W. E. & Schwandt, P. C. Amplification of synaptic current by persistent sodium conductance in apical dendrite of neocortical neurons. *J. Neurophysiol.* **74**, 2220–2224 (1995).
- Stuart, G. & Sakmann, B. Amplification of EPSPs by axosomatic sodium channels in neocortical pyramidal neurons. *Neuron* **15**, 1065–1076 (1995).
- Spencer, W. A. & Kandel, E. R. Electrophysiology of hippocampal neurons. IV. Fast pre-potentials. *J. Neurophysiol.* **24**, 272–285 (1961).
- Wong, R. K., Prince, D. A. & Basbaum, A. I. Intracellular recordings from hippocampal neurons. *Proc. Natl Acad. Sci. USA* **76**, 986–990 (1979).
- Benardo, L. S., Masukawa, L. M. & Prince D. A. Electrophysiology of isolated hippocampal pyramidal dendrites. *Neuroscience* **2**, 1614–1622 (1982).
- Regehr, W., Kehoe, J. S., Ascher, P. & Armstrong, C. Synaptically triggered action potentials in dendrites. *Neuron* **11**, 145–151 (1993).
- Andreasen, M. & Lambert J. D. Regenerative properties of pyramidal cell dendrites in area CA1 of the rat hippocampus. *J. Physiol. (Lond.)* **483**, 421–441 (1995).
- Stuart, G. J. & Sakmann B. Active propagation of somatic action potentials into neocortical pyramidal cell dendrites. *Nature* **367**, 69–72 (1994).
First clear-cut evidence for active propagation of action potentials in the dendrites of neocortical neurons.

55. Stuart, G., Spruston, N., Sakmann, B. & Häusser, M. Action potential initiation and backpropagation in neurons of the mammalian CNS. *Trends Neurosci.* **20**, 125–131 (1997).
56. Magee, J. C. & Johnston, D. A synaptically controlled, associative signal for Hebbian plasticity in hippocampal neurons. *Science* **275**, 209–213 (1997).
57. Linden, D. J. The return of the spike: postsynaptic action potentials and the induction of LTP and LTD. *Neuron* **22**, 661–666 (1999).
58. Stuart, G., Schiller, J. & Sakmann, B. Action potential initiation and propagation in rat neocortical pyramidal neurons. *J. Physiol. (Lond.)* **505**, 617–632 (1997).
59. Schwandt, P. C. & Crill, W. E. Local and propagated dendritic action potentials evoked by glutamate iontophoresis on rat neocortical pyramidal neurons. *J. Neurophysiol.* **77**, 2466–2483 (1997).
60. Schwandt, P. C. & Crill, W. E. Synaptically evoked dendritic action potentials in rat neocortical pyramidal neurons. *J. Neurophysiol.* **79**, 2432–2446 (1998).
61. Golding, N. L. & Spruston, N. Dendritic sodium spikes are variable triggers of axonal action potentials in hippocampal CA1 pyramidal neurons. *Neuron* **21**, 1189–1200 (1998).
62. Wei, D.-S. *et al.* Compartmentalized and binary behavior of terminal dendrites in hippocampal pyramidal neurons. *Science* **193**, 2272–2275 (2001).
63. Williams, S. R. & Stuart, G. J. Dependence of EPSP efficacy on synapse location in neocortical pyramidal neurons. *Science* **295**, 1907–1910 (2002).
64. Hines, M. L. & Carnevale, N. T. The NEURON simulation environment. *Neural Comput.* **9**, 1179–1209 (1997).
65. London, M. & Segev, I. Synaptic scaling *in vitro* and *in vivo*. *Nature Neurosci.* **4**, 853–855 (2001).
66. Paré, D., Lebel, E. & Lang, E. J. Differential impact of miniature synaptic potentials on the somata and dendrites of pyramidal neurons *in vivo*. *J. Neurophysiol.* **78**, 1735–1739 (1997).
67. Salinas, E. & Sejnowski, T. J. Impact of correlated synaptic input on output firing rate and variability in simple neuronal models. *J. Neurosci.* **20**, 6193–6209 (2000).
68. Tiesinga, P. H. E., José, J. V. & Sejnowski, T. J. Comparison of current-driven and conductance-driven neocortical model neurons with Hodgkin-Huxley voltage-gated channels. *Phys. Rev. E* **62**, 8413–8419 (2000).
69. Destexhe, A., Rudolph, M., Fellous, J. M. & Sejnowski, T. J. Fluctuating conductances recreate *in vivo*-like activity in neocortical neurons. *Neuroscience* **107**, 13–24 (2001).
70. Lin, J. K., Pawelzik, K., Ernst, U. & Sejnowski, T. J. Irregular synchronous activity in stochastically-coupled networks of integrate-and-fire neurons. *Network* **9**, 333–344 (1998).
71. Brunel, N. & Hakim, V. Fast global oscillations in networks of integrate-and-fire neurons with low firing rates. *Neural Comput.* **11**, 1621–1671 (1999).
72. Diesmann, M., Gewaltig, M.-O. & Aertsen, A. Stable propagation of synchronous spiking in cortical neural networks. *Nature* **402**, 529–533 (1999).
73. Wang, X. J. Synaptic basis of cortical persistent activity: the importance of NMDA receptors to working memory. *J. Neurosci.* **19**, 9587–9603 (1999).
74. Brunel, N. Persistent activity and the single-cell frequency-current curve in a cortical network model. *Network* **11**, 261–280 (2000).
75. Brunel, N. Dynamics of sparsely connected networks of excitatory and inhibitory spiking neurons. *J. Comp. Neurosci.* **8**, 183–208 (2000).
76. Compte, A., Brunel, N., Goldman-Rakic, P. S. & Wang, X. J. Synaptic mechanisms and network dynamics underlying spatial working memory in a cortical network model. *Cereb. Cortex* **10**, 910–923 (2000).
77. Timofeev, I., Grenier, F., Bazhenov, M., Sejnowski, T. J. & Steriade, M. Origin of slow cortical oscillations in deafferented cortical slabs. *Cereb. Cortex* **10**, 1185–1199 (2000).
78. Compte, A., Sanchez-Vives, M. V., McCormick, D. A. & Wang, X. J. Cellular and network mechanisms of slow oscillatory activity (<1 Hz) and wave propagations in a cortical network model. *J. Neurophysiol.* **89**, 2707–2725 (2003).
79. Shelley, M., McLaughlin, D., Shapley, R. & Wielaard, J. States of high conductance in a large-scale model of the visual cortex. *J. Comput. Neurosci.* **13**, 93–109 (2002).
80. London, M., Schreibleman, A., Häusser, M., Larkum, M. E. & Segev, I. The information efficacy of a synapse. *Nature Neurosci.* **5**, 332–340 (2002).
81. Hö, N. & Destexhe, A. Synaptic background activity enhances the responsiveness of neocortical pyramidal neurons. *J. Neurophysiol.* **84**, 1488–1496 (2000).
- Theoretical study investigating the effect of synaptic noise on neuronal responsiveness. This was the first demonstration of the contrasting effects of conductance and noise with a suggested link to an attentional mechanism.**
82. Wiesenfeld, K. & Moss, F. Stochastic resonance and the benefits of noise: from ice ages to crayfish and SQUIDS. *Nature* **373**, 33–36 (1995).
83. Doiron, B., Longtin, A., Berman, N. & Maler, L. Subtractive and divisive inhibition: effect of voltage-dependent inhibitory conductances and noise. *Neural Comput.* **13**, 227–248 (2000).
84. Longtin, A., Doiron, B. & Bulsara, A. R. Noise-induced divisive gain control in neuron models. *Biosystems* **67**, 147–156 (2002).
85. Stacey, W. C. & Durand, D. M. Synaptic noise improves detection of subthreshold signals in hippocampal CA1 neurons. *J. Neurophysiol.* **86**, 1104–1112 (2001).
- First experimental evidence that synaptic noise can improve signal detection in central neurons.**
86. Rudolph, M. & Destexhe, A. Do neocortical pyramidal neurons display stochastic resonance? *J. Comput. Neurosci.* **11**, 19–42 (2001).
87. Segev, I., Rinzler, J. & Shepherd, G. M. *The Theoretical Foundation of Dendritic Function: Selected Papers of Wilfrid Rall with Commentaries* (MIT Press, Cambridge, Massachusetts, 1995).
88. Magee, J. C. & Cook, E. P. Somatic EPSP amplitude is independent of synapse location in hippocampal pyramidal neurons. *Nature Neurosci.* **3**, 895–903 (2000).
- Experimental and theoretical study of hippocampal pyramidal neurons showing evidence that the conductance of individual excitatory synapses is scaled according to distance from soma, therefore compensating for dendritic cable filtering.**
89. Rudolph, M., Hö, N. & Destexhe, A. Synaptic background activity affects the dynamics of dendritic integration in model neocortical pyramidal neurons. *Neurocomputing* **38**, 327–333 (2001).
90. Rudolph, M. & Destexhe, A. The discharge variability of neocortical neurons during high-conductance states. *Neuroscience* **119**, 855–873 (2003).
91. Rudolph, M. & Destexhe, A. Gain modulation and frequency locking under conductance noise. *Neurocomputing* **52**, 907–912 (2003).
92. Halliday, D. M. Weak, stochastic temporal correlation of large-scale synaptic inputs is a major determinant of neuronal bandwidth. *Neural Comput.* **12**, 693–707 (1999).
93. Rudolph, M. & Destexhe, A. Correlation detection and resonance in neural systems with distributed noise sources. *Phys. Rev. Lett.* **86**, 3662–3665 (2001).
94. Vaadia, E. *et al.* Dynamics of neuronal interactions in monkey cortex in relation to behavioural events. *Nature* **373**, 515–518 (1995).
- First experimental demonstration that pairs of neurons can be linked to behavioural changes by modulating the correlation of their firing, with no change in their average firing rate.**
95. deCharms, R. C. & Merzenich, M. M. Primary cortical representation of sounds by the coordination of action-potential timing. *Nature* **381**, 610–613 (1996).
96. Riehle, A., Grün, S., Diesmann, M. & Aertsen, A. Spike synchronization and rate modulation differentially involved in motor cortical function. *Science* **278**, 1950–1953 (1997).
97. Rudolph, M. & Destexhe, A. Tuning neocortical pyramidal neurons between integrators and coincidence detectors. *J. Comput. Neurosci.* **14**, 239–251 (2003).
98. Krüger, J. & Becker, J. D. Recognizing the visual stimulus from neuronal discharges. *Trends Neurosci.* **14**, 282–286 (1991).
99. Häusser, M. & Clark, B. A. Tonic synaptic inhibition modulates neuronal output pattern and spatiotemporal synaptic integration. *Neuron* **19**, 665–678 (1997).
100. Harsch, A. & Robinson, P. C. Postsynaptic variability of firing in rat cortical neurons: the roles of input synchronization and synaptic NMDA receptor conductance. *J. Neurosci.* **20**, 6181–6192 (2000).
101. Kislley, M. A. & Gerstein, G. L. The continuum of operating modes for a passive model neuron. *Neural Comput.* **11**, 1139–1154 (1999).
102. Marsálek, P., Koch, C. & Maunsell, J. On the relationship between synaptic input and spike output jitter in individual neurons. *Proc. Natl Acad. Sci. USA* **94**, 735–740 (1997).
103. Mel, B. W. Information processing in dendritic trees. *Neural Comput.* **6**, 1031–1085 (1994).
104. Shadlen, M. N. & Newsome, W. T. The variable discharge of cortical neurons: implications for connectivity, computation, and information coding. *J. Neurosci.* **18**, 3870–3896 (1998).
105. Stevens, C. F. & Zador, A. M. Input synchrony and the irregular firing of cortical neurons. *Nature Neurosci.* **1**, 210–217 (1998).
106. Mainen Z. F. & Sejnowski, T. J. Reliability of spike timing in neocortical neurons. *Science* **268**, 1503–1506 (1995).
107. Sharp, A. A., O’Neil, M. B., Abbott, L. F. & Marder, E. The dynamic clamp: artificial conductances in biological neurons. *Trends Neurosci.* **16**, 389–394 (1993).
108. Robinson, H. P. & Kawai, N. Injection of digitally synthesized synaptic conductance transients to measure the integrative properties of neurons. *J. Neurosci. Methods* **49**, 157–165 (1993).
109. Chance, F. S., Abbott, L. F. & Reyes, A. D. Gain modulation from background synaptic input. *Neuron* **15**, 773–782 (2002).
110. Fellous, J. M., Rudolph, M., Destexhe, A. & Sejnowski, T. J. Synaptic background noise controls the input/output characteristics of single cells in an *in vitro* model of *in vivo* activity. *Neuroscience* (in the press).
111. Prescott, S. A. & De Koninck, Y. Gain control of firing rate by shunting inhibition: roles of synaptic noise and dendritic saturation. *Proc. Natl Acad. Sci. USA* **100**, 2076–2081 (2003).
112. Hasenstaub, A. R., Shu, Y. S., Badoual, M., Bal, T. & McCormick, D. A. The effects of recurrent activity on the responsiveness of cortical neurons to synaptic inputs. *Soc. Neurosci. Abstr.* **753.4** (2002).
113. Salinas, E. & Thier, P. Gain modulation: a major computational principle of the central nervous system. *Neuron* **27**, 15–21 (2000).
114. Steriade M. Ascending control of thalamic and cortical responsiveness. *Int. Rev. Neurobiol.* **12**, 87–144 (1970).
115. Singer, W., Treter, F. & Cynader, M. The effect of reticular stimulation on spontaneous and evoked activity in the cat visual cortex. *Brain Res.* **102**, 71–90 (1976).
116. Treue, S. & Trujillo, C. M. Feature-based attention influences motion processing gain in macaque visual cortex. *Nature* **399**, 575–579 (1999).
117. Markram, H., Lübke, J., Frotscher, M., Roth, A. & Sakmann, B. Physiology and anatomy of synaptic connections between thick tufted pyramidal neurones in the developing rat neocortex. *J. Physiol. (Lond.)* **500**, 409–440 (1997).
118. Rudolph, M. & Destexhe, A. Characterization of subthreshold voltage fluctuations in neuronal membranes. *Neural Comput.* (in the press).
119. Dean, A. The variability of discharge of simple cells in the cat striate cortex. *Exp. Brain Res.* **44**, 437–440 (1981).
120. Holt, G. R., Softky, W. R., Koch, C. & Douglas, R. J. Comparison of discharge variability *in vitro* and *in vivo* in cat visual cortex neurons. *J. Neurophysiol.* **75**, 1806–1814 (1996).

Acknowledgements

We thank M. Badoual, T. Bal, M. Steriade and I. Timofeev for intracellular recording data. Research supported by the Centre National de la Recherche Scientifique (France), Future and Emerging Technologies (European Union), the Human Frontier Science Program and the National Institutes of Health.